European Congress on Computational Methods in Applied Sciences and Engineering
ECCOMAS 2000
Barcelona, 11-14 September 2000

EFFICIENT SOLVING OF MECHANICAL PROBLEMS WITH MESHLESS METHODS : DOMAIN DECOMPOSITION AND QUADRATURE SCHEME

P. Breitkopf[*], A. Rassineux[*], J-M Savignat[†] and P. Villon[*]

[*] Universite de Technologie de Compiegne
BP 20529, 60205 Compiegne cedex, France
e-mail: Piotr.Breitkopf@utc.fr

[†] CGES, Ecole Nationale Supérieure des Mines de Paris
35, rue Saint Honoré
77305 Fontainebleau Cedex, France

Key words: Meshless methods, Moving Least Squares Approximation, Patch Test, Numerical Integration

Abstract. *This paper concerns current researches on meshless methods alternative to finite elements. Two issues are defined as crucial at the current state of development of the family of meshless methods based on the variational formulation of governing equations:*

1. *In the absence of an explicit mesh, the influence domains for each node have to be construncted in a way to obtain following properties of the resulting shape functions:*
   - *regularity*
   - *simplicity of support*
2. *The method of integration has to satisfy the patch test.*

The work approaches both problems in a global manner. The proposed idea relies on the decomposition of the domain into a set of tiled rectangles. The domain of influence of each node is then defined as a set of such tiles. The assembly procedure for the global stiffness matrix is conducted successively for each tile. The basic integration unit is a tile and a standard Gauss-Legendre integration scheme is used.

This approach is tested with Diffuse Element Method (DEM).

1 INTRODUCTION

This paper concerns solving partial differential equations using the Moving Least Squares (MLS) approximation with a variational formulation. The idea is to replace the finite element shape functions by their MLS equivalents and reuse as much as possible the standard finite element framework. However, several issues have to be treated with special attention:

- In the absence of an explicit mesh, one has to define the subdomains of integration for the evaluation of the elementary matrices;
- The domains of influence of MLS shape functions have to coincide with integration subdomains.

We propose a tessellation scheme which uses a relatively small numbers of rectangular and triangular subdomains. The numerical results are discussed using the linear patch test and an example problem.

2 MOVING LEAST SQUARES APPROXIMATION

The MLS approximation is the basis of the family of such meshless formulations as the Generalized Finite Difference Method (GFDM)[1], Diffuse Element Method (DEM)[2], Element Free Galerkin (EFG)[3] or the Finite Point method (FP)[4]. In this section we recall the basic features of the MLS:

- the MLS approximation provides smooth approximations of function values across irregular grids of data points;
- it is local : at any arbitrary evaluation point $\mathbf{x}$, only the closest nodes $\mathbf{x}_i$ are taken into account;
- the influence of a node $\mathbf{x}_i$ is governed by a decreasing weight function $w_i = w(\mathbf{x}_i, \mathbf{x})$ which vanishes outside the domain of influence of the node $\mathbf{x}_i$;

Given a column vector of nodal function values $\mathbf{u}(\mathbf{x}_i)$, the value $u(\mathbf{x})$ is given by

$$u(\mathbf{x}) = \mathbf{N}^{\mathbf{T}}(\mathbf{x})\mathbf{u}(\mathbf{x}_i) \tag{1}$$

In the usual presentation of the MLS the shape functions $\mathbf{N}$ are

$$\mathbf{N}^{\mathbf{T}} = \mathbf{p(x)A}^{-1}\mathbf{B} \tag{1}$$

where $\mathbf{p}$ is a vector of base functions, usually polynomials

$$\mathbf{p}=\langle 1xy\ldots\rangle \tag{3}$$

and the matrices $\mathbf{A}$ and $\mathbf{B}$ are

$$\begin{aligned}\mathbf{A}&=\sum_{\mathbf{i}}\mathbf{p}^{\mathbf{T}}(\mathbf{x_i})w_i\mathbf{p}(\mathbf{x_i})\\ \mathbf{B}&=\left[\cdots\quad w_i\mathbf{p}^{\mathbf{T}}(\mathbf{x_i})\quad\cdots\right]\end{aligned} \tag{4}$$

The computation of the derivative of $\mathbf{N}$ is more complex form than that of the function itself

$$\begin{aligned}\mathbf{N'^{T}(x)}=\mathbf{p'(x)A^{-1}B}+\mathbf{p(x)}\left(\mathbf{(A^{-1})'B}+\mathbf{A^{-1}B'}\right)=\\ \mathbf{p'(x)A^{-1}B}+\mathbf{p(x)A^{-1}}\left(\mathbf{B'}-\mathbf{A'A^{-1}}\right)\end{aligned} \tag{5}$$

so that the above expression is sometimes approximated by its first term

$$\dot{\mathbf{N}}^{\mathbf{T}}=\mathbf{p'A^{-1}B} \tag{6}$$

called "diffuse derivative" $\dot{\mathbf{N}}$ as opposed to the "full derivative" $\mathbf{N'(x)}$.

As shown[5], the diffuse derivative often provides a very good approximation of the derivative and it converges towards the full derivative of the approximation.

The explicit form of the MLS shape functions given in 1D is given in[6]

$$N_i=\frac{\sum_{j\neq i}w_iw_j(x-x_j)(x_i-x_j)}{d},\quad d=\sum_{i=1,n-1}\sum_{j=i+1,n}w_iw_j(x_i-x_j)^2 \tag{7}$$

The full derivative is

$$\begin{aligned}N_i'&=\frac{1}{d}\sum_{j\neq i}w_iw_j(x_i-x_j)+\frac{1}{d}\sum_{j\neq i}(w_{i,x}w_j+w_iw_{j,x})(x-x_j)(x_i-x_j)-N_i\frac{d'}{d}\\ d'&=\sum_{i=1,n-1}\sum_{j=i+1,n}(w_{i,x}w_j+w_iw_{j,x})(x_i-x_j)^2\end{aligned} \tag{8}$$

while the diffuse derivative reduces to:

$$\dot{N}_i = \frac{1}{d} \sum_{j \neq i} w_i w_j \left(x_i - x_j \right) \tag{9}$$

Equivalent expressions for 2D and 3D are given in the same work[6].

3 DOMAIN DISCRETIZATION

The common feature of the family of meshless methods based on MLS approximations is obtained when replacing the finite element shape functions by their MLS equivalents. Several issues which do not arise in the finite element method have to be solved.

In the finite element method, the continuum Ω is divided into a finite number (say E) of open disjoint subregions – finite elements $\{\Omega_e, e=1,2,\ldots,E\}$ such that $\Omega_e \cap \Omega_f = \Phi$ for $e \neq f$. The finite elements serve as integration cells for numerical evaluation of the global integrals over the domain Ω, generally using the Gauss-Legendre scheme.

In meshless methods, the evaluation of integrals over Ω depends on the way in which we define the influence domains of the nodes. Two strategies are possible:

- at each evaluation point we take into account k closest nodes – we will refer this method as the *R(x)* strategy;
- the domains of influence are arbitrarily fixed by assigning a radius of influence to each node which we call the $r(x)$ strategy.

The *R(x)* strategy guarantees the existence of the MLS approximation at each evaluation point belonging to Ω. The Figure 1(a) illustrates the domains of influence for a regular grid of nodes with k=4. The individual integration cells are then given by the Voronoï diagram of 4-th order – polygons defined by the sets of points having the same list of 4 closest neighboring nodes.

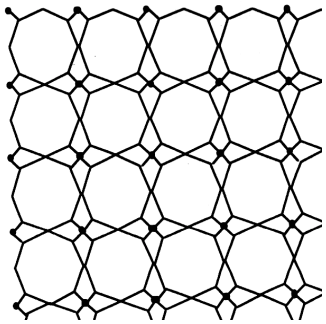

Figure 1(a)

Fourth order Voronoï diagram Integration cells with R(x)strategy on a regural grid of nodes; nodes are denoted by thick points

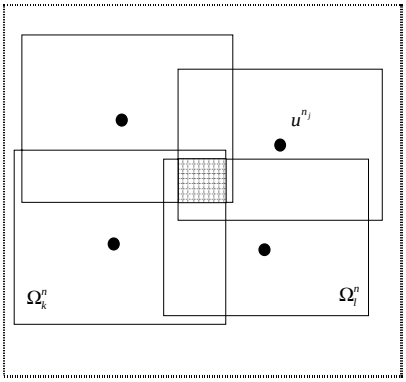

Figure 1(b)

Integration cells with $n(x)$ strategy are simpler, but their number is still important

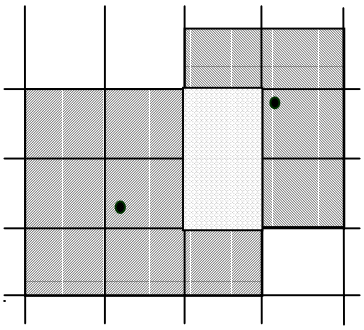

Figure 1(c)

When domains of influence from Figure 1(b) are aligned with a predefined tessellation, the integration cells correspond to individual tessels

It is easily seen that the shape of the integration domains is complex even on the regular grid of nodes. Moreover, the computational complexity of high order Voronoï diagrams is prohibitive. On the other hand, the generation of a finite element mesh requires only a first order Voronoï diagram and one would be tempted to use such a background finite element mesh for the numerical integration purposes. Besides the fact that the method looses its "meshless" character, other problems are encountered with this approach principaly due to changes in the number of connected nodes across the elements.

The $n(x)$ strategy permits to simplify the shapes of the domains of influence of the nodes. In the Figure 2 we show the domains of influence in the L^2 and L^∞ norms. In our work we choose the L^∞ norm as it gives simpler domains.

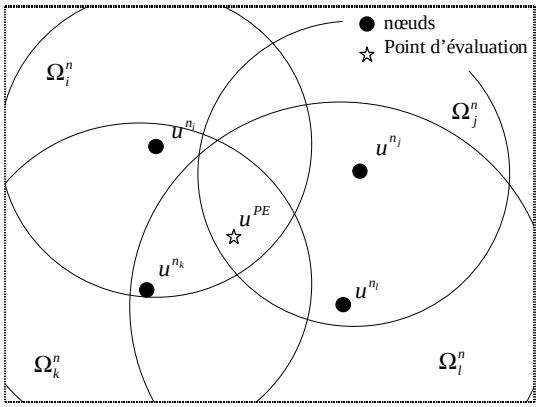

Figure 2a

Domains of influence in L^2 norm.

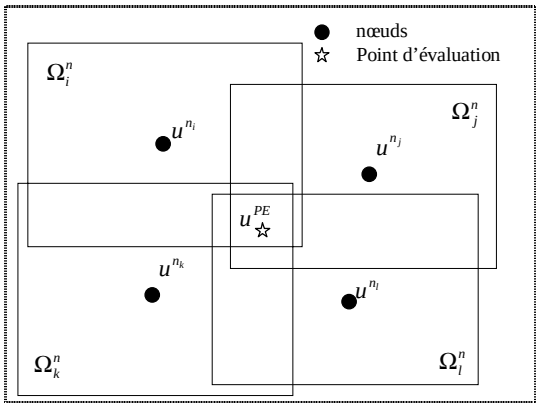

Figure 2b

Domains of influence in L^∞ norm

The Figure 1(b) shows a typical integration domain given by intersection of four domains of influence. The difficulty when using the $n(x)$ strategy consists in satisfying the two contradictory requirements:

- the domains of influence have to big enough in order to guarantee the existence of the approximation in each point of Ω;
- the domains of influence should be as small as possible in order to limit the bandwith of the resulting global system.

The second requirement governs also the accuracy of the approximation. It may be shown that these conditions are satisfied with the procedure shown in Figure 3(a): first, we build the first order Voronoï diagram and then, for each node we create the domain of influence as a rectangular envelope of Voronoï cells surrounding the cell to which the node belongs. We note that the node is not centered in the resultaing domain of influence.

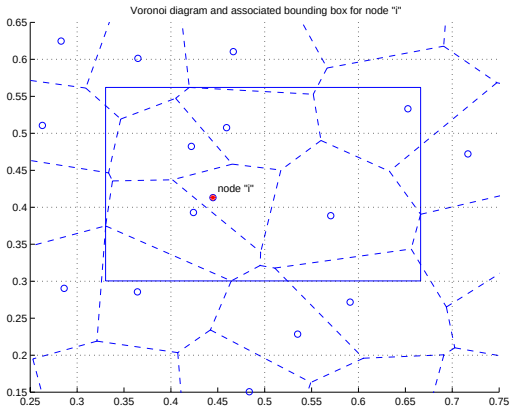

Figure 3(a)

Domain of influence defined as an envelope of surrounding Voronoï cells

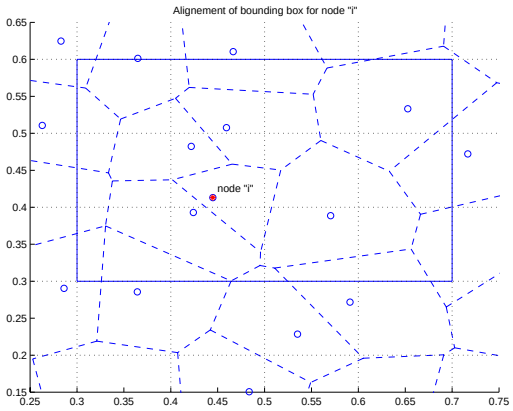

Figure 3(b)

Domain of influence expanded to fit the tessellation grid

In order to diminish the number of integration subregions we define a tessellation of the domain. The tessellation grid may be regular or adjusted locally to the average size of the Voronoï cells. The domains of influence corresponding to the Figure 3(a) are further expanded to match the tessellation grid. As each nodal domain of influence consists of a set of tessels, so the intesection between two domains is given also by a set of tessels. The list of connected nodes is constant over a tessel. The Figure 1(c) illustrates the further simplification of the form of the integration cells and the decrease of their number.

The Figure 5 shows a typical interpolating shape function and its derivatives over an asymmetric domain.

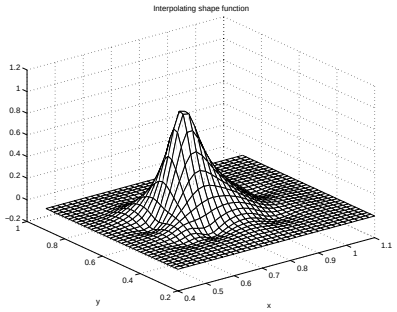

Figure 5(a)

Shape function over an asymmetric domain

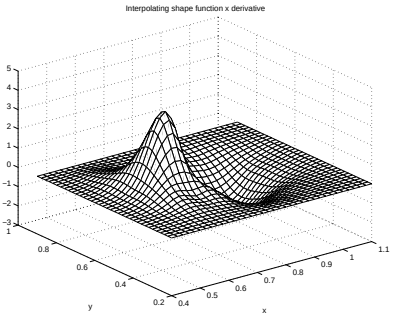

Figure 5(b)

Shape function x derivative over an asymmetric domain

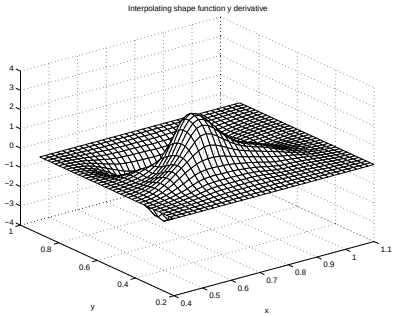

Figure 5(c)

Shape function y derivative over an asymmetric domain

4 NUMERICAL INTEGRATION AND THE PATCH TEST

The obvious choice for the numerical integration is the usual Gauss Legendre scheme. The integration points for rectangular are directly obtained by standard mapping from the reference domain. The cells intersected by the boundary $\partial\Omega$ have more complex forms and have to be treated separately. For these cases, an isoparametric mapping may be used in the same way as in the finite elements. Another solution consists in subdividing the boundary tessels into simpler, triangular and rectangular forms. In Figure 6, the green tessels correspond to internal integration cells and the yellow ones belong to the discretized boundary tessels.

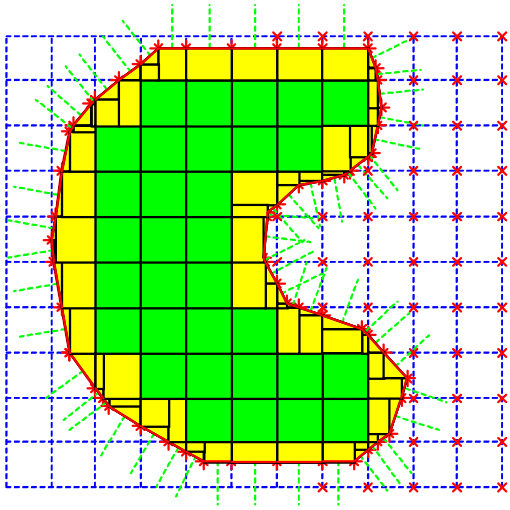

Figure 6

Internal (green) and boundary (yellow) integration cells

In the patch test the displacements are prescribed along all outside boundaries of a domain by a linear function of the coordinates[7]. The strains and stresses in this case should be constant. When a numerical method solving the partial differential equations fulfills this condition, we say that it passes the patch test. This approach to test the numerical formulation an the code itself is standard in the finite element method. In the following section, we use our tessellation scheme along with the DEM and EFG formulations. The details of the test problem may be found in[7]. The boundary conditions are enforced using the modified variational principle[8].

The figures 7(a) and 7(b) illustrate the convergence of the patch test on a unit square for

orders of standard Gauss integration varying from 1 to 12, and different number of integration cells, MLS with full and with diffuse derivative. Three conclusions may be drawn:

- in both cases the patch test is not *a priori* satisfied;
- for the complete derivative, the patch test is satisfied independently of the tessellation density, when refining the numerical integration;
- the diffuse derivative performs poorly, independently of the tessellation density and of the number of Gauss points.

The first two points are easily explained when considering (7). As opposed to the finite elements, the MLS shape functions do not have the polynomial form. In fact, for the weights *w* given by the spline functions, the MLS shape functions are rational fractions whose order is defined by the number of connected nodes and by the order of the polynomial expression of $w(\mathbf{x},\mathbf{x}_i)$. Therefore, the integration is not well performed by the classical Gauss-Legendre scheme.

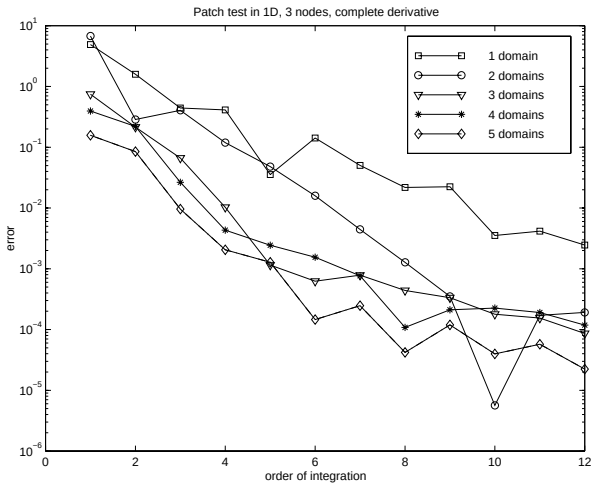

Figure 7(a)

Convergence of the patch test on a unit square for varying orders of standard Gauss integration and different number of integration cells, MLS with full derivative

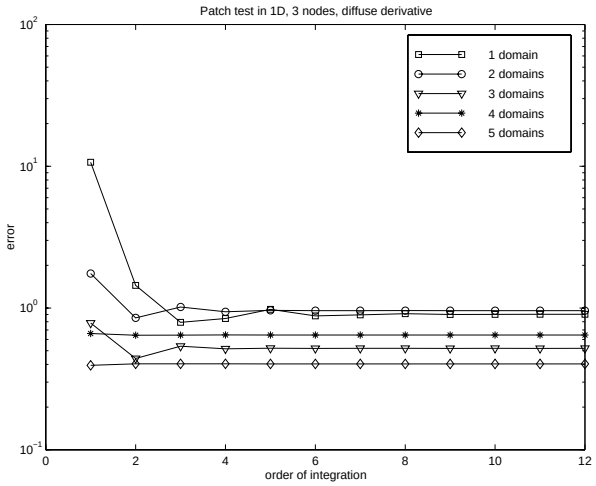

Figure 7(b)

Convergence of the patch test on a unit square for varying orders of standard Gauss integration and different number of integration cells, MLS with diffuse derivative

The convergence of the patch test is then explained by the convergence of the numerical integration itself. The failure of the diffuse derivative in variational formulation is less obvious to explain. This behavior is opposite to that observed for strong formulations based on finite differences on irregular grids[1,9], where the diffuse derivation performs well.

In the second example (Figure 8), we analyze the convergence of the patch test with

different numbers of nodes, and we compare again the full and diffuse derivatives. We observe that both formulations converge at approximately the same rate for high numbers of nodes. The obtained precision is however not acceptable when considering the computational cost and the precision for the diffuse derivative is still significantly worse.

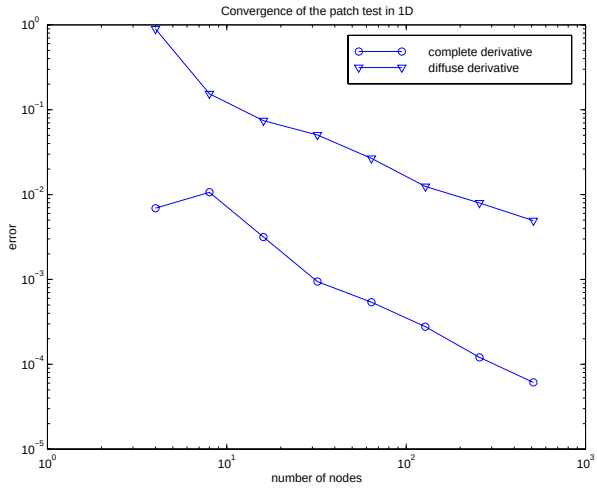

Figure 8

Convergence of the patch test with varying number of nodes, comparison of the full and diffuse derivatives.

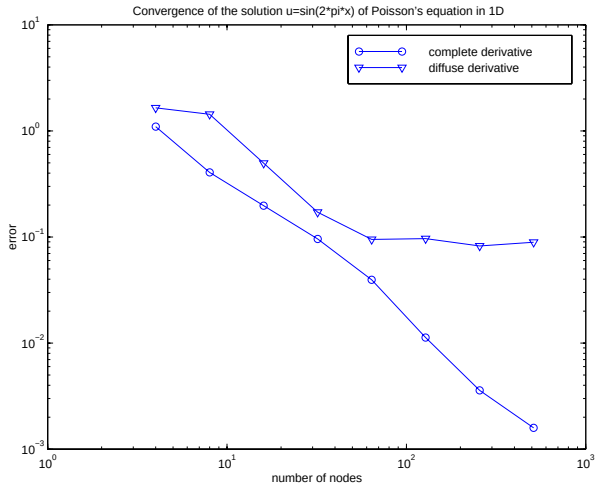

Figure 9

Convergence of the solution of Poisson equation with varying number of nodes, comparison of the full and diffuse derivatives.

The Figure 9 gives the results for the same domain as used for the patch test, but the equation solved and the boundary conditions are chosen now to give the exact solution *u=sin(2*pi*x)*. We see, that the full derivative version performs reasonably well, while the diffuse derivative diverges.

5 CONCLUSIONS

The proposed discretization scheme satisfies the patch test at convergence for increasing number of numerical integration points and for increasing number of nodes. The full derivative has to be used. Similar results are obtained when solving an example problem. The principal drawback of the method is that the patch test is not satisfied exactly for low number of nodes and for low number of integration points. The reason is probably the form of the shape functions expressions. The rational fractions with high degree are poorly integrated by the Gauss Legendre method.

Actually, we are working on the development of a custom quadrature scheme for MLS shape functions in order to ensure the properties needed for exact verification of the patch test.

REFERENCES

[1] Liszka T., Orkisz J., *The Finite Difference Method at Arbitrary Irregular Grids and its Applied Mechanics*, Comp.and Struct., **11**, 83-95, (1980).

[2] Nayroles B., Touzot G., Villon P., *Generalizing the Finite Element Method: Diffuse Approximation and Diffuse Elements*, Computational Mechanics, **10**, 307-318. (1992).

[3] Belytschko T., Lu Y.Y., Gu L., *Element-free Galerkin Methods*, Intern.Journ.for Numer.Meth.in Engng, **37**, 229-256, (1994).

[4] Onate E., Idelsohn S., Zienkiewicz O.C., Taylor R.L., *A Finite Point Method in Computational Mechanics. Applications to Convective Transport and Fluid Flow*, Int. J. for Numerical Meth. In Engng, **39**, 3839-3886, (1996).

[5] Lancaster P., Salkauskas K., *Curve and Surface Fitting: an Introduction,* Academic Press, London, Orlando, **1986**

[6] P. Breitkopf, A. Rassineux, G. Touzot, P. Villon, *Explicit form and efficient computation of MLS shape functions and their derivatives*, International Journal for Numerical Methods in Engineering, in print, **47**, (2000).

[7] Lu Y.Y., Belytschko T., Gu L., *A New Implementation of the Element Free Galerkin Method*, Computer Meth. In Applied Mechanics and Engng, **113**, 397-414, (1994).

[8] Y.X. Mukherjee, S.Mukherjee, *On boundary conditions in element-free Galerkin Maethod*, Computational Mechanics, **11**, 264-270, (1997)..

[9] P. Breitkopf, G. Touzot, P. Villon *Consistency Approach and Diffuse Derivation in Element Free Methods Based on Moving Least Squares Approximation*, Computer Assisted Mechanics and Engineering Sciences, **5**, 479-501, (1998).